

Exact statistics and thermodynamic uncertainty relations for a  
periodically driven electron pump

Non Peer-reviewed author version

Harunari, Pedro E.; Fiore, Carlos E. & PROESMANS, Karel (2020) Exact statistics and thermodynamic uncertainty relations for a periodically driven electron pump. In: Journal of Physics A-Mathematical and Theoretical, 53 (37) (Art N° 374001).

DOI: 10.1088/1751-8121/aba05e

Handle: <http://hdl.handle.net/1942/32992>

# Exact statistics and thermodynamic uncertainty relations for a periodically driven electron pump

Pedro E. Harunari<sup>1</sup>, Carlos E. Fiore<sup>1</sup> and Karel Proesmans<sup>2,3</sup>

<sup>1</sup> Institute of Physics of São Paulo University, Rua do Matão, 1371, 05508-090 São Paulo, SP, Brazil

<sup>2</sup> Simon Fraser University, 8888 University Drive, Burnaby, British Columbia, Canada

<sup>3</sup> Hasselt University, B-3590 Diepenbeek, Belgium

E-mail: [pedro.harunari@usp.br](mailto:pedro.harunari@usp.br)

**Abstract.** We introduce a model for a periodically driven electron pump that sequentially interacts with an arbitrary number of heat and particle reservoirs. Exact expressions for the thermodynamic fluxes, such as entropy production and particle flows are derived arbitrarily far from equilibrium. We use the present model to perform a comparative study of thermodynamic uncertainty relations that are valid for systems with time-periodic driving.

## 1. Introduction

Over the last few decades, stochastic thermodynamics has emerged as a theory to describe the thermodynamic properties of mesoscopic systems using Markov dynamics [1, 2]. It not only reproduces the fundamental results from classical thermodynamics, but also introduces several new concepts, such as the Jarzynski equality [3, 4], the thermodynamics of information processing [5], the thermodynamics of phase transitions [6, 7, 8, 9, 10], an extension of linear irreversible thermodynamics to time-periodic systems [11, 12, 13, 14, 15] and others. Furthermore, technological advancements have opened up the possibility to probe these theoretical predictions on real microscopic systems [16, 17, 18, 19].

Recently, a general bound, known as the thermodynamic uncertainty relations (TUR) has been derived [20, 21, 22, 23, 24, 25] following its proposal in the context of biomolecular processes [26]. It shows for steady-state Markov systems that the signal to noise ratio of any thermodynamic flux is bounded by half the entropy production rate. Such a relationship has been used to infer the entropy production rate [27, 28, 29, 30] and to bound the performance of mesoscopic heat engines [31]. Furthermore, it has been verified experimentally [32, 33], linked to the fundamental symmetries of the system [34, 35, 36], and several extensions to other thermodynamic observables have been derived [37, 38]. One can however show that the original TUR does not hold for systems with time-periodic driving [39, 40, 41]. Several extensions of the original TUR have been proposed [42, 43, 44, 45, 46, 47], raising the question of how tight they are and how they perform in different regimes. Such a quantitative comparison has however not been done.

One of the drawbacks concerning the study of periodically driven systems is that the number of exactly solvable models is rather limited [48, 49, 50, 51]. One notable exception is the electron pump model, derived by Rosas et al. [52, 53]. In this model, a two-level system is sequentially brought into contact with two or three reservoirs, which allows for the transfer of electrons between those reservoirs. Due to the simplicity of a two-level system, it is possible to derive analytic results [54, 55, 56]. Here, we extend those results to a model with an arbitrary number of reservoirs.

One of the strengths of this model is that one has full access to all relevant quantities, such as number of thermodynamic fluxes, their affinities and the driving period. Therefore, it is possible to look at several regimes, such as the near equilibrium regime (where the thermodynamic fluxes can be determined from the Onsager coefficients) and the regime where one of the affinities is much larger than the others. This flexibility makes the system the perfect toy model to do a quantitative comparison of the time-periodic thermodynamic uncertainty relations.

This paper is organized as follows. In Sec. 2 we describe the model and show how the solutions from [52, 53] can be extended to an arbitrary number of reservoirs. These results are used in Sec. 3 to study the stochastic thermodynamics of our model. In Sec. 4, we give an overview of the existing thermodynamic uncertainty relations for

time-periodic systems. We compare those uncertainty relations in the context of the electron pump model in Sec. 5. Finally, our conclusions are discussed in Sec. 6.

## 2. Model and exact solution

The model under study consists of a single-level quantum dot, that can be empty or occupied by a single electron. The quantum dot is sequentially placed in contact with one of the  $N$  electron reservoirs for a duration  $\tau'$ , after which it is decoupled from that reservoir and coupled to the next one, c.f. Fig. 1. The total period of one cycle is  $\tau = N\tau'$ , after which the system returns to its initial configuration and electrons may have been transferred between the reservoirs.

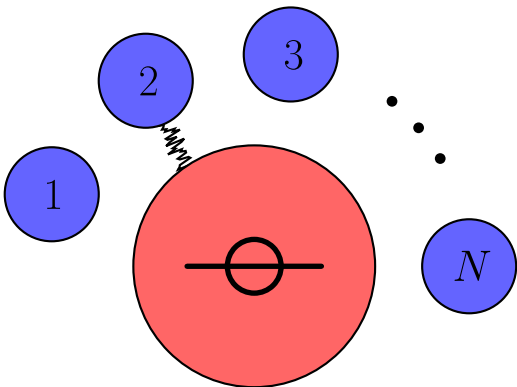


**Figure 1.** Description of the system composed of a quantum dot in contact with reservoir 2. After an amount of time  $\tau'$ , the quantum dot will be decoupled from reservoir 2 and coupled to reservoir 3.

When the quantum dot is in contact with a given reservoir, its dynamics is described by the master equation

$$\dot{p}(t) = \omega(t)(1 - p(t)) - \bar{\omega}(t)p(t), \quad (1)$$

where  $p(t)$  denotes the probability of the quantum dot being occupied by an electron at time  $t$  and  $\omega(t)$  and  $\bar{\omega}(t)$  denote the transition rates for an electron to jump from the reservoir to the system and vice versa. Throughout this paper we shall assume that the quantum dot is always in contact with a single reservoir with constant jump rates, i.e., jump rates are  $\omega(t) = \omega_i$  and  $\bar{\omega}(t) = \bar{\omega}_i$  when  $t \in [(i-1)\tau', i\tau'[$  and  $i \in \{1, \dots, N\}$ .

Since two-level systems coupled to a single reservoir relax to an equilibrium state, the probability of the quantum dot being occupied by an electron when it is in contact with only one reservoir  $i$  converges to

$$p_i^{eq} \equiv \frac{\omega_i}{\omega_i + \bar{\omega}_i}. \quad (2)$$

This will no longer be true when the quantum dot is periodically connected to different reservoirs for a finite amount of time. In that case, the reservoirs exchange electrons

and the system continuously produces entropy. One can however find the occupation probability by solving the master equation Eq. (1) explicitly, which leads to

$$p(t) = p_i^{\text{eq}} + [p((i-1)\tau') - p_i^{\text{eq}}] e^{-(\omega_i + \bar{\omega}_i)(t - (i-1)\tau')}, \quad (3)$$

where the value of the integer  $i$  in the right-hand side is the one which satisfies  $(i-1)\tau' \leq t < i\tau'$ , i.e., it is the index of the reservoir that is interacting with the quantum dot at time  $t$ .  $p(t)$  is the exact time-periodic occupation probability of the quantum dot. With this information we can evaluate all macroscopic quantities of interest. Since the system is ergodic and is driven time-periodically, it relaxes to a time-periodic steady-state distribution  $p^{\text{ss}}(t + \tau) = p^{\text{ss}}(t)$  [57], which can be obtained solely in terms of the transition rates and the length of the period:

$$p^{\text{ss}}(t) = p_i^{\text{eq}} + e^{-(\omega_i + \bar{\omega}_i)(t - (i-1)\tau')} \times \left\{ \frac{\xi_{1,i-1}}{1 - \xi_{1,N}} \left[ \Delta_{N,1} + \sum_{n=2}^N \xi_{n,N} \Delta_{n-1,n} \right] + \sum_{m=2}^i \xi_{m,i-1} \Delta_{m-1,m} \right\}, \quad (4)$$

where we introduced  $\Delta_{i,j} \equiv p_i^{\text{eq}} - p_j^{\text{eq}}$  and  $\xi_{i,j} \equiv \exp\{-\tau' \sum_{n=i}^j (\omega_n + \bar{\omega}_n)\}$ . Throughout the paper, we will always assume that the system has reached its time-periodic steady state. We pause to make a few comments. First, a time-independent equilibrium distribution is recovered when  $\Delta$ 's vanish. Second, the above general expression reduces to the results derived in Refs. [52] and [53] for  $N = 2$  and 3 respectively. Third, in the limit of strong coupling,  $\omega_i, \bar{\omega}_i \rightarrow \infty$  for all  $i$ ,  $p^{\text{ss}}(t)$  essentially corresponds to an equilibrium distribution  $p_i^{\text{eq}}$ .

We shall now calculate the electron flux out of reservoir  $i$ . This corresponds to the difference between the occupancy  $n(t)$  at the beginning and at the end of the interaction divided by the period,  $J_i \equiv [n(i\tau') - n((i-1)\tau')]/\tau$ , where the occupancy  $n(t) = 1$  if the quantum dot is occupied at time  $t$  and  $n(t) = 0$  otherwise. By taking the average of  $J_i$ , we arrive at the following expression

$$\begin{aligned} \bar{J}_i &= \frac{p^{\text{ss}}(i\tau') - p^{\text{ss}}((i-1)\tau')}{\tau} \\ &= \frac{1}{\tau} \left\{ \frac{\xi_{1,i-1}}{1 - \xi_{1,N}} \left[ \Delta_{N,1} + \sum_{n=2}^N \xi_{n,N} \Delta_{n-1,n} \right] + \sum_{m=2}^i \xi_{m,i-1} \Delta_{m-1,m} \right\} (\xi_{i,i} - 1), \end{aligned} \quad (5)$$

where the overline represents the ensemble average.

One can easily check that this expression satisfies the property  $\sum_{i=1}^N \bar{J}_i = 0$ , as would be expected. Furthermore, one can also derive an expression for the variance of

the flux per cycle  $\text{var}(J_i) \equiv \tau \left( \overline{J_i^2} - \overline{J_i}^2 \right)$ :

$$\begin{aligned} \text{var}(J_i) &= \frac{\overline{[n(i\tau') - n((i-1)\tau')]^2} - \overline{[n(i\tau') - n((i-1)\tau')]^2}}{\tau} \\ &= \frac{1 - \xi_{i,i}}{\tau} 2p_i^{\text{eq}}(1 - p_i^{\text{eq}}) \\ &\quad + \frac{1 - \xi_{i,i}}{\tau} (1 - 2p_i^{\text{eq}}) \left\{ \frac{\xi_{1,i-1}}{1 - \xi_{1,N}} \left[ \Delta_{N,1} + \sum_{n=2}^N \xi_{n,N} \Delta_{n-1,n} \right] + \sum_{m=2}^i \xi_{m,i-1} \Delta_{m-1,m} \right\} \\ &\quad - \frac{(1 - \xi_{i,i})^2}{\tau} \left\{ \frac{\xi_{1,i-1}}{1 - \xi_{1,N}} \left[ \Delta_{N,1} + \sum_{n=2}^N \xi_{n,N} \Delta_{n-1,n} \right] + \sum_{m=2}^i \xi_{m,i-1} \Delta_{m-1,m} \right\}^2, \quad (6) \end{aligned}$$

where we used the properties  $\overline{n(i\tau')n((i-1)\tau')} = p^{\text{ss}}(i\tau'|n((i-1)\tau')=1)p^{\text{ss}}((i-1)\tau')$ ,  $\overline{n(i\tau')} = \overline{n(i\tau')^2} = p^{\text{ss}}(i\tau')$  and Eqs. (1), (3) and (4).

### 3. Stochastic Thermodynamics

Having defined the dynamics of the system, we are now ready to introduce its stochastic thermodynamics [1, 2, 58]. In particular, we can define the chemical work flux  $\dot{W}_i^{(\text{chem})}$  and the heat flux  $\dot{Q}_i(t)$  associated with the  $i$ -th reservoir,

$$\dot{W}_i^{(\text{chem})}(t) = \mu_i \dot{p}(t), \quad (7)$$

$$\dot{Q}_i(t) = (\epsilon - \mu_i) \dot{p}(t), \quad (8)$$

for  $t$  satisfying  $(i-1)\tau' \leq t < i\tau'$ . Here, we have defined the chemical potential of the  $i$ -th reservoir  $\mu_i$  and the energy of the quantum dot  $\epsilon$ . As we are assuming the energy level of the quantum dot to be constant, the mechanical work delivered to the system will be zero. Using the definitions of the electron fluxes, one can also determine the total average delivered amount of chemical work and produced heat per cycle in the steady state:

$$\overline{\dot{W}}^{(\text{chem})} = \sum_{i=1}^N \overline{J}_i \mu_i = \sum_{i=2}^N \overline{J}_i (\mu_i - \mu_1), \quad (9)$$

and

$$\overline{\dot{Q}} = \sum_{i=1}^N \overline{J}_i (\epsilon - \mu_i) = \sum_{i=2}^N \overline{J}_i (\mu_1 - \mu_i), \quad (10)$$

where in both cases we used  $\sum_i \overline{J}_i = 0$ .

Due to the periodicity of the system, one has  $\overline{\dot{Q}} = -\overline{\dot{W}}^{(\text{chem})}$ , in agreement with the first law of thermodynamics.

The entropy production rate, averaged over one period, can be determined using Schnakenberg's formula [59]:

$$\overline{\Pi} = \frac{1}{\tau} \sum_{i=1}^N \int_{(i-1)\tau'}^{i\tau'} [\omega_i - (\omega_i + \overline{\omega}_i) p^{\text{ss}}(t)] \ln \frac{\omega_i (1 - p^{\text{ss}}(t))}{\overline{\omega}_i p^{\text{ss}}(t)} dt, \quad (11)$$

where the Boltzmann constant is set to unity here and hereafter.

Taking into account the periodicity of  $p(t)$ , the mean entropy production per unit of time, averaged over one cycle,  $\bar{\Pi}$  can be rewritten to a sum of fluxes  $\bar{J}_i$  and associated thermodynamic forces  $X_i$

$$\bar{\Pi} = \sum_{i=2}^N \bar{J}_i X_i, \quad (12)$$

where  $\bar{J}_i$  is given by Eq. (5) and the forces  $X_i$  read

$$X_i \equiv \ln \frac{\omega_i \bar{\omega}_1}{\bar{\omega}_i \omega_1}. \quad (13)$$

This structure for the entropy production rate is a well-known result from classical non-equilibrium thermodynamics [60, 61]. The first reservoir is regarded as a reference, so the thermodynamic forces are quantified by how much they drive the system away from the reference system, similar to [52, 53].

By taking into account the local detailed balance assumption, the entropy production formula can also be rewritten in terms of the heat fluxes:

$$\frac{\omega_i}{\bar{\omega}_i} = e^{-(\epsilon - \mu_i)/T_i}, \quad (14)$$

which gives an expression for the transition rates in terms of the macroscopic variables  $\mu_i$ ,  $\epsilon$  and the  $i$ -th reservoir's temperature  $T_i$ . Furthermore, the thermodynamic forces  $X_i$  can now also be related to

$$X_i = \frac{\epsilon - \mu_1}{T_1} - \frac{\epsilon - \mu_i}{T_i}. \quad (15)$$

By combining Eqs. (10), (12) and (15), we re-obtain the classical thermodynamic definition for the mean entropy production

$$\bar{\Pi} = \sum_{i=1}^N \frac{\bar{Q}_i}{T_i}. \quad (16)$$

Finally, we mention that it is also possible to apply a near-equilibrium approach to this system, in which Onsager coefficients and reciprocal relations are derived. This will be done in Appendix A.

#### 4. Time-periodic thermodynamic uncertainty relations

Generically, Thermodynamic Uncertainty Relations (TURs) impose bounds between fluctuations of a given flux and the associated dissipation rate. In its original formulation it states that for an ergodic system described by a time independent Markov dynamics, the steady state currents (e.g. flux of particles or heat) obey a trade-off between signal and noise. The signal corresponds to the long-time limit of an instantaneous current  $\langle j_t \rangle$  – that considers the jumps in time  $t$  and their weights such as privileged directions in

the state space – averaged over all possible stochastic trajectories  $\langle j \rangle = \lim_{t \rightarrow \infty} \langle j_t \rangle / t$ . Conversely, the noise is given by its variance  $\text{Var}(j) = \lim_{t \rightarrow \infty} (\langle j_t^2 \rangle - \langle j_t \rangle^2) / t$  and the dissipation can be identified with the long-time limit of the instantaneous entropy production rate  $\sigma = \lim_{t \rightarrow \infty} \Sigma_t / t$ .

The existence of a universal bound relating above observables was conjectured by Barato et al. [26] and afterwards proven from the tools of large deviation theory [62] by Gingrich et al. [22] and Pietzonka et al. [21]. It states that

$$\frac{\sigma \text{Var}(j)}{2k_B \langle j \rangle^2} \geq 1. \quad (17)$$

Several works [41, 42, 44, 45, 46, 47, 63] have shown that this bound no longer holds in the presence of time-dependent driving and hence Eq. (17) generally will not be valid for the electron pump discussed previously. For this reason, we will look at extensions of Eq. (17). In the next subsections we provide a concise overview of them. Although these bounds hold for any flux in the system, we shall cast them in terms of the particle fluxes into the reservoirs, cf. Eqs. (5) and (6).

#### 4.1. Effective entropy production relation

A first extension was proposed by Koyuk et al. in Ref. [44] and corresponds to a generalization of the original TUR [20]:

$$\frac{\text{Var}(J_i) \bar{\Pi}_{\text{eff}}}{2\bar{J}_i^2} \geq 1, \quad (18)$$

where it takes into account the thermodynamic cost of the periodic driving of the system by a small modification in the standard entropy production rate, namely the effective entropy production  $\bar{\Pi}_{\text{eff}}$ . In the case of the electron pump, it is given by

$$\bar{\Pi}_{\text{eff}} \equiv \frac{1}{\tau} \sum_{i=1}^N \int_{(i-1)\tau}^{i\tau} \frac{(\omega_i - (\omega_i + \bar{\omega}_i)p^{\text{eff}})^2}{\omega_i - (\omega_i + \bar{\omega}_i)p^{\text{ss}}(t)} \ln \left[ \frac{(1 - p^{\text{ss}}(t))\omega_i}{p^{\text{ss}}(t)\bar{\omega}_i} \right] dt, \quad (19)$$

where in the present case  $p^{\text{eff}} \equiv \tau^{-1} \int_0^\tau p^{\text{ss}}(t) dt$  is the average occupancy of the quantum dot over one steady-state cycle. Note that above expression reduces to the Eq. (11) when the steady-state is time-independent  $p^{\text{ss}}(t) = p^{\text{eff}}$ .

#### 4.2. Generalized entropy production relation

A number of different generalizations of the TUR for time-periodic systems have been proposed by Barato et al. [46]. Their validity depend on individual properties such as the time-dependence and symmetries presented in the increment of the current. Particularly suited for the present model is the TUR given by (cf. GTUR4 in [46])

$$\frac{\text{Var}(J_i)}{2\bar{J}_i^2} C_a(p^{\text{eff}}) \geq 1, \quad (20)$$



that has the form of Eq. (17) and for the present model

$$C_a(p) \equiv \frac{2}{\tau} \sum_{i=1}^N \int_{(i-1)\tau}^{i\tau} \frac{[(1-p)\omega_i - p\bar{\omega}_i]^2}{(1-p^{\text{ss}}(t))\omega_i - p^{\text{ss}}(t)\bar{\omega}_i} dt, \quad (21)$$

where  $p$  is a number between 0 and 1. Here, we set  $p \rightarrow p^{\text{eff}} \equiv \tau^{-1} \int_0^\tau p^{\text{ss}}(t) dt$  as introduced in Section 4.1. This relation is generally tighter than Eq. (18) [46].

### 4.3. Hysteretic relation

The third TUR to be considered was derived in [45], it relates the fluxes of the system in "forward" and "backward" (time-inverted driving) directions. More specifically, it takes into account the sum of the fluxes (and their variances) under forward and time-reversed drivings [45, 64]. Such a "hysteretic" TUR satisfies a bound similar to the one derived for time-symmetric driving [42] and reads

$$\frac{(\text{Var}(J_i) + \text{Var}(\tilde{J}_i)) \left( e^{\tau(\bar{\Pi} + \tilde{\Pi})/2k_B} - 1 \right)}{\tau(\bar{J}_i + \tilde{J}_i)^2} \geq 1, \quad (22)$$

where  $\tilde{J}_i$ ,  $\tilde{J}_i^2$  and  $\tilde{\Pi}$  stand for the results under time-inverted driving, which can be appraised in terms of transition rates

$$\tilde{\omega}(t) \equiv \omega(\tau - t) \quad \text{and} \quad \tilde{\bar{\omega}}(t) \equiv \bar{\omega}(\tau - t). \quad (23)$$

In our case, it corresponds to inverting the sequence of reservoirs to which the system is coupled.

### 4.4. Driving frequency relation

The fourth and last TUR we shall look at is a bound introduced by Koyuk et al. [47], also referred as driving frequency relation, since it takes into account the response of the current to a change in the driving period. More specifically the driving frequency TUR states that

$$\frac{\bar{\Pi} \text{Var}(J_i)}{2(\bar{J}_i + \tau \frac{\partial \bar{J}_i}{\partial \tau})^2} \geq 1. \quad (24)$$

One advantage of this TUR is that it consists of quantities with clear macroscopic interpretations, that can be directly evaluated from the (forward) time dynamics.

## 5. Comparing time-periodic thermodynamic uncertainty relations

We are now in position to apply the aforementioned TURs to the present system. The analysis will be divided in three parts: firstly, in Figs. 2 and 3, we shall compare them for fixed periods and distinct model parameters for the three and five stage cases. We

will scale all thermodynamic forces  $X_i$ 's with a control parameter  $x$ . This gives us the possibility to study the near equilibrium regime when  $x \approx 0$  and the far from equilibrium regime,  $x \rightarrow \pm\infty$ . Secondly, Fig. 4 depicts, for the five stage case, the situation where one thermodynamic force is much smaller/larger than the others. More precisely, we keep all thermodynamic forces apart from  $X_4$  fixed and analysis is undertaken for distinct values of  $X_4$ . Finally, in Figs. 5 and 6, we study the dependency of the TURs on the period of the driving. In all cases, we shall focus on the TURs applied to the particle fluxes  $J_i$  into each reservoir  $i$ .

In Figs. 2 and 3, one can see that the TURs are indeed valid, as expected. Furthermore, they seem to converge to a similar value near equilibrium,  $x \approx 0$ , although divergences might occur when the denominators in the TUR go to zero (for example when the average flux  $\bar{J}_i$  vanishes). Furthermore, for most fluxes, the TURs seem more tight near equilibrium. One can also easily check that, although the TURs seem to have a qualitatively similar behaviour over a broad range of parameters there is no TUR which is uniformly better than the others. The behavior of an electron pump with three reservoirs, Fig. 2, is qualitatively similar to the behaviour of the electron pump with five reservoirs, Fig. 3. Finally, one can see that the correct choice of flux is important if one wants to infer the entropy production rate from the TUR. For example, in Fig. 2, one can see that the bound for  $J_3$  is reasonably tight in general, but the bound for  $J_1$  is off by a factor 100 over a broad range of parameters.

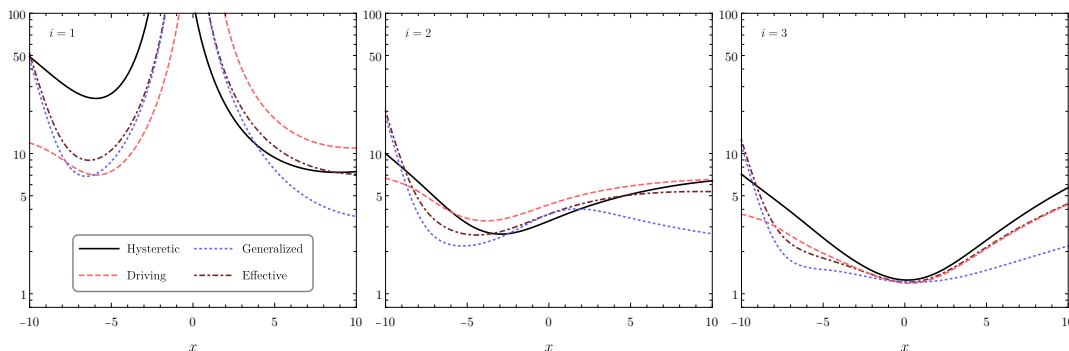


**Figure 2.** Curves represent the LHS of TURs in Eqs. (18) (brown dot-dashed line), (20) (blue dotted line), (22) (black full line) and (24) (pink dashed line) for the electron flux  $J_i$ , associated with reservoir  $i$  ( $i = 1, 2, 3$ ). These quantities need to be  $\geq 1$  to satisfy each TUR. We consider the three stage electron pump versus parameter  $x$  with affinities  $X_1 = 0$ ,  $X_2 = 0.2x$  and  $X_3 = -0.5x$ . For  $x = 0$  the system is at the equilibrium regime. Other parameters:  $\omega_1 = \bar{\omega}_1 = 0.3$ ,  $\bar{\omega}_2 = 0.8$ ,  $\bar{\omega}_3 = 0.2$  and  $\tau = 1$ . Except for  $i = 1$ ,  $\omega_i$ ,  $\bar{\omega}_i$  and  $X_i$  are related from Eq. (13).

This can also be seen in Fig. 4, where one only varies  $X_4$ . If  $X_4$  is small, the TURs associated with  $J_4$  are generally less tight, while the TURs associated with the other reservoirs are tighter. Meanwhile, the TURs associated with  $J_4$  seem to become tighter for larger  $X_4$ . The reason for this is that for large  $X_4$ , the entropy production is

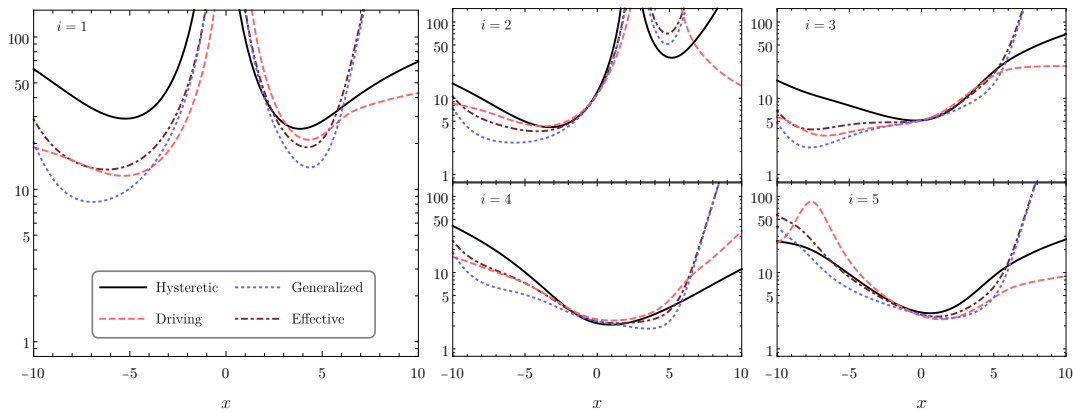


**Figure 3.** Curves represent the LHS of TURs in Eqs. (18) (brown dot-dashed line), (20) (blue dotted line), (22) (black full line) and (24) (pink dashed line) for the electron flux  $J_i$ , associated with reservoir  $i$  ( $i = 1, 2, 3, 4, 5$ ). These quantities need to be  $\geq 1$  to satisfy each TUR. We consider the five stage electron pump versus parameter  $x$  with affinities  $X_1 = 0$ ,  $X_2 = 0.2x$ ,  $X_3 = -0.5x$ ,  $X_4 = 0.7x$  and  $X_5 = -0.4x$ . For  $x = 0$  the system is at the equilibrium regime. Other parameters:  $\omega_1 = \bar{\omega}_1 = 0.3$ ,  $\bar{\omega}_2 = 0.8$ ,  $\bar{\omega}_3 = 0.2$ ,  $\bar{\omega}_4 = 0.3$ ,  $\bar{\omega}_5 = 0.5$  and  $\tau = 1$ . Except for  $i = 1$ ,  $\omega_i$ ,  $\bar{\omega}_i$  and  $X_i$  are related from Eq. (13).

dominated by the contact with the 4-th reservoir. Therefore, one can get a good estimate of the total entropy production, or a tight thermodynamic uncertainty relation, by just looking at the 4th flux. On the other hand, all other fluxes become small compared to the entropy production, meaning that the TURs associated to the other fluxes become loose.

Finally in Figs. 5 and 6, we study the dependency of the TURs on the period of the driving. From expressions of  $\bar{J}_i$ ,  $\text{Var}(J_i)$ ,  $\bar{\Pi}$ ,  $\bar{\Pi}_{\text{eff}}$  and  $C_a(p_{\text{eff}})$ , it is possible to find the asymptotic behaviors of TURs for sufficiently slow and fast periods. In fact they acquire the asymptotic behaviors for large  $\tau$

$$\bar{J}_i \sim \frac{1}{\tau}, \quad \text{Var}(J_i) \sim \frac{1}{\tau}, \quad \bar{\Pi} \sim \frac{1}{\tau}, \quad \bar{\Pi}_{\text{eff}} \sim 1, \quad C_a(p_{\text{eff}}) \sim 1, \quad \ln \left| \bar{J}_i + \tau \frac{\partial \bar{J}_i}{\partial \tau} \right| \sim -\tau. \quad (25)$$

This implies that the TURs (18) and (20) diverge linearly and Eq. (24) exponentially as  $\tau$  is increased, whereas the hysteretic TUR, Eq. (22), remains finite. Conversely, for  $\tau \rightarrow 0$  all of above quantities remain finite, hence all TURs are limited in the slow driving regime, even though they can take very large values.

## 6. Conclusions

We studied the nonequilibrium properties of a single-particle stochastic pump sequentially placed in contact with an arbitrary number of reservoirs. Exact expressions for fluxes and thermodynamic quantities are found arbitrarily far from equilibrium. We

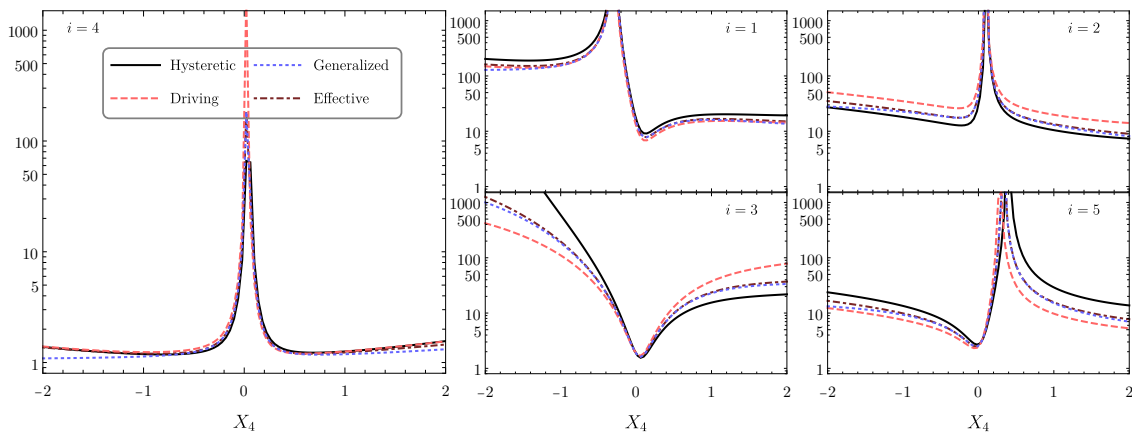


**Figure 4.** Curves represent the LHS of TURs in Eqs. (18) (brown dot-dashed line), (20) (blue dotted line), (22) (black full line) and (24) (pink dashed line) for the electron flux  $J_i$ , associated with reservoir  $i$  ( $i = 1, 2, 3, 4, 5$ ). These quantities need to be  $\geq 1$  to satisfy each TUR. We consider the five stage electron pump versus the affinity related to the fourth reservoir  $X_4$ . The others are  $X_1 = 0$ ,  $X_2 = 0.05$ ,  $X_3 = -0.1$  and  $X_5 = 0.1$ . The larger panel depicts the TUR associated with the fourth reservoir. Far from the origin the system is in the regime of one of the affinities being much larger than the others. Also, we considered  $\omega_1 = \bar{\omega}_1 = 0.3$ ,  $\bar{\omega}_2 = 0.8$ ,  $\bar{\omega}_3 = 0.2$ ,  $\bar{\omega}_4 = 0.3$ ,  $\bar{\omega}_5 = 0.5$  and  $\tau = 1$ . Except for  $i = 1$ ,  $\omega_i$ ,  $\bar{\omega}_i$  and  $X_i$  are related from Eq. (13).

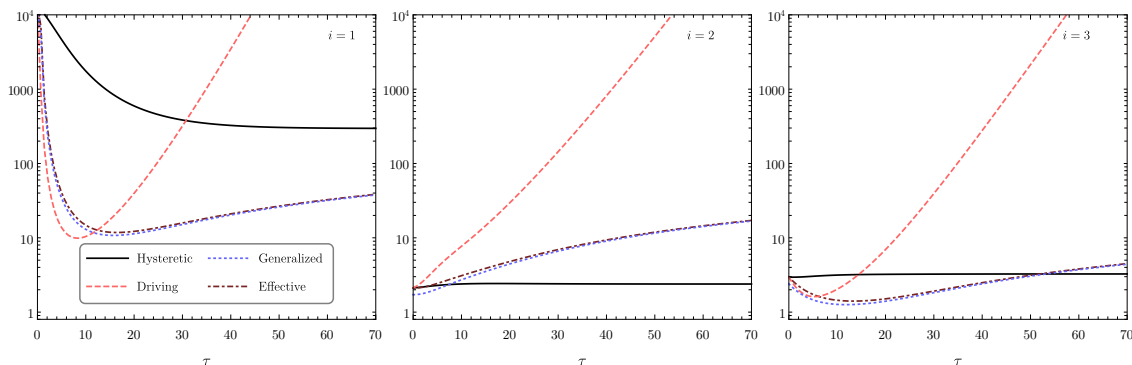


**Figure 5.** Curves represent the LHS of TURs in Eqs. (18) (brown dot-dashed line), (20) (blue dotted line), (22) (black full line) and (24) (pink dashed line) for the electron flux  $J_i$ , associated with reservoir  $i$  ( $i = 1, 2, 3$ ). These quantities need to be  $\geq 1$  to satisfy each TUR. We consider the three stage electron pump versus period  $\tau$  with affinities  $X_1 = 0$ ,  $X_2 = -2$  and  $X_3 = 1.25$ . Other parameters:  $\omega_1 = \bar{\omega}_1 = 0.7$ ,  $\bar{\omega}_2 = 0.3$  and  $\bar{\omega}_3 = 0.1$ . Except for  $i = 1$ ,  $\omega_i$ ,  $\bar{\omega}_i$  and  $X_i$  are related from Eq. (13).

tested and verified several TURs for time-periodic systems. Near equilibrium, all TURs yield similar results, but far from equilibrium their tightness often differ by several orders of magnitude. Furthermore, there is no TUR that seems to be uniformly better than the others. One can however verify that in the slow-driving limit all TURs, except for the hysteretic TUR Eq. (22), become arbitrarily loose. It would be interesting to check whether this conclusion is true for more general periodically driven systems. Inferring quantities such as the average flux or the entropy production rate from these TURs

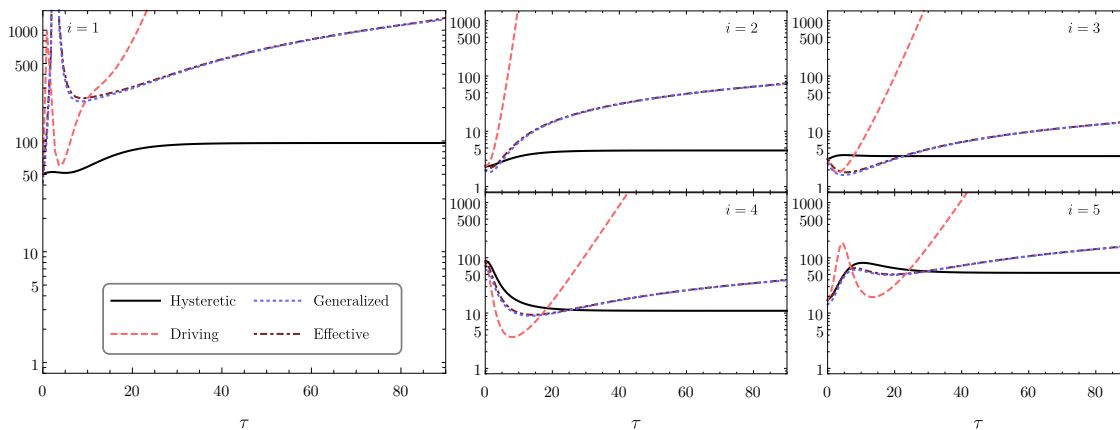


**Figure 6.** Curves represent the LHS of TURs in Eqs. (18) (brown dot-dashed line), (20) (blue dotted line), (22) (black full line) and (24) (pink dashed line) for the electron flux  $J_i$ , associated with reservoir  $i$  ( $i = 1, 2, 3$ ). These quantities need to be  $\geq 1$  to satisfy each TUR. We consider the five stage electron pump versus period  $\tau$  with affinities  $X_1 = 0$ ,  $X_2 = 1.8$ ,  $X_3 = -1.5$ ,  $X_4 = 0.7$ ,  $X_5 = -0.4$ ,  $\omega_1 = \bar{\omega}_1 = 0.7$ ,  $\bar{\omega}_2 = 0.3$ ,  $\bar{\omega}_3 = 0.8$ ,  $\bar{\omega}_4 = 0.2$  and  $\bar{\omega}_5 = 0.5$ . Except for  $i = 1$ ,  $\omega_i$ ,  $\bar{\omega}_i$  and  $X_i$  are related from Eq. (13).

seems inaccurate, since TURs for individual fluxes often differ from their lower bounds by orders of magnitude. It would be interesting to see whether one can overcome this issue by looking at combined fluxes, which might lead to hyperaccurate currents for which the TUR becomes tight [30].

## 7. Acknowledgements

C. E. F. and P. E. H. acknowledge the financial support from FAPESP under grants No 2018/02405-1 and 2017/24567-0, respectively.

## Appendix A. Linear regime and Onsager coefficients

In this appendix, we derive the reciprocal relations for the system exposed to an arbitrary number of sequential reservoirs. In the absence of odd parity variables, Onsager coefficients generally satisfy the so called Onsager reciprocal relations,  $L_{ij} = L_{ji}$ . This is no longer the case for systems with time-dependent drivings, since the time-reversal symmetry is broken in such a case. For continuous time periodic drivings, Onsager symmetry is replaced by the weaker Onsager-Casimir reciprocal relation, which relates the Onsager coefficients under time-forward driving to the cross-coefficient of time-reversed driving,

$$L_{ij} = \tilde{L}_{ji}, \quad (\text{A.1})$$

where  $\tilde{L}$  attempts to the reversed driving. Since we are dealing with a distinct type of periodically driven system, Eq. (A.1) has to be updated in order to incorporate the

sequential exposure and hence a different structure for reciprocal relations is expected. From the linear expansion of the mean current  $\bar{J}_i$  [Eq. (5)], we have that  $L_{i,j}$  reads

$$L_{i,j} = \left. \frac{\partial \bar{J}_i}{\partial X_j} \right|_{\text{eq}} = \nu_j \left. \frac{\partial \bar{J}_i}{\partial \nu_j} \right|_{\text{eq}}, \quad (\text{A.2})$$

where we introduced the quantity  $\nu_i = \omega_i/\bar{\omega}_i$  and the subscript ‘‘eq’’ refers to the equilibrium case in which  $X_i = 0$  (or  $\nu_i = \nu, \forall i$ ). For  $j \leq i$  and  $m = \{1, 2, \dots, N\}$  they are then given by

$$L_{i,j} = \frac{(1 - \xi_{j,j})(\xi_{1,i-1}\xi_{j+1,N} + \xi_{j+1,i-1}(1 - \xi_{1,N})) + \delta_{i,j}(1 - \xi_{1,N})(\xi_{j,j} - 2)}{1 - \xi_{1,N}} \times \left. \frac{(\xi_{i,i} - 1)\nu_j}{\tau(\nu_j + 1)^2} \right|_{\nu_m \rightarrow \nu} \quad (\text{A.3})$$

and for  $j > i$  and  $m = \{1, 2, \dots, N\}$  they are

$$L_{i,j} = \frac{\xi_{1,i-1}(1 - \xi_{j,j})\xi_{j+1,N}}{1 - \xi_{1,N}} \left. \frac{(\xi_{i,i} - 1)\nu_j}{\tau(\nu_j + 1)^2} \right|_{\nu_m \rightarrow \nu}. \quad (\text{A.4})$$

Above expressions are held valid for an arbitrary number of reservoirs  $N$ . Taking for instance the forward protocol and its reverse order as sketched in Fig. A1, the time reversal consists of inverting the order of reservoir exposures. Since the process is cyclic, it can be accomplished by taking the backward sequence  $\{N, N - 1, \dots, 1\}$ , in which the  $N$ -th reservoir plays the role of reference in the reversed dynamics, so the equilibrium probability of occupation is now given by  $p_N^{\text{eq}}$ .

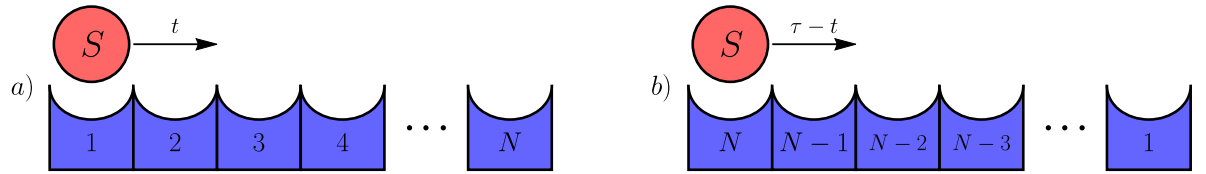


**Figure A1.** Illustration of the sequence of reservoirs that interacts with the system at each interval  $\tau/N$  in a cycle. a) is the forward protocol while b) is the time-reversed one.

Thereby, the reciprocal relation for an arbitrary number of sequential reservoirs reads

$$L_{i,j} = \tilde{L}_{\tilde{j},\tilde{i}}, \quad (\text{A.5})$$

with  $\tilde{i} = N + 1 - i$ ,  $\tilde{j} = N + 1 - j$ , the  $i$ -th and  $j$ -th reservoir under time-inverted driving, for  $i, j = 1, \dots, N$ . The Onsager matrix is symmetric in relation to the Onsager matrix for the time-reversed dynamics.

The time reversal symmetry then corresponds to perform the transformation  $i \rightarrow \tilde{j}$  and  $j \rightarrow \tilde{i}$  and hence the function  $\xi_{i,j}$  becomes

$$\xi_{i,j} \rightarrow \xi_{\tilde{j},\tilde{i}}. \quad (\text{A.6})$$

For  $j < i$  the right side in Eq. (A.3) reads

$$\tilde{L}_{\tilde{j},\tilde{i}} = \left[ \frac{(1 - \xi_{N-i+1,N-i+1})(\xi_{N-i+2,N}\xi_{1,N-j} + \xi_{N-i+2,N-j}(1 - \xi_{1,N}))}{1 - \xi_{1,N}} \times \frac{(\xi_{N-j+1,N-j+1} - 1)\nu_{N-i+1}}{\tau(\nu_{N-i+1} + 1)^2} \right]_{\text{eq}} \quad (\text{A.7})$$

$$= \frac{(1 - \xi_{i,i})(\xi_{j+1,N}\xi_{1,i-1} + \xi_{j+1,i-1}(1 - \xi_{1,N}))}{1 - \xi_{1,N}} \frac{(\xi_{j,j} - 1)\nu}{\tau(\nu + 1)^2} \Big|_{\text{eq}} = L_{i,j}. \quad (\text{A.8})$$

Analogous result can be obtained for  $i \leq j$ . With these results for  $\tilde{L}_{\tilde{j},\tilde{i}}$  in the cases  $j < i$  and  $i \leq j$ , (A.5) is analytically verified. This then completes our proof about the appropriate reciprocal relations for the present case. The above result is valid for an arbitrary number of reservoirs.

## Bibliography

- [1] Seifert U 2012 *Reports on progress in physics* **75** 126001
- [2] Van den Broeck C and Esposito M 2015 *Physica A: Statistical Mechanics and its Applications* **418** 6–16
- [3] Jarzynski C 1997 *Physical Review Letters* **78** 2690
- [4] Jarzynski C 2011 *Annual review of condensed matter physics* **2** 329–351
- [5] Parrondo J M, Horowitz J M and Sagawa T 2015 *Nature physics* **11** 131–139
- [6] Noa C F, Harunari P E, de Oliveira M and Fiore C 2019 *Physical Review E* **100** 012104
- [7] Herpich T, Thingna J and Esposito M 2018 *Physical Review X* **8** 031056
- [8] Herpich T and Esposito M 2019 *Physical Review E* **99** 022135
- [9] Campisi M and Fazio R 2016 *Nature communications* **7** 1–5
- [10] Goes B O, Fiore C E and Landi G T 2020 *Physical Review Research* **2** 013136
- [11] Brandner K, Saito K and Seifert U 2015 *Physical review X* **5** 031019
- [12] Proesmans K and Van den Broeck C 2015 *Physical review letters* **115** 090601
- [13] Proesmans K, Cleuren B and Van den Broeck C 2016 *Journal of Statistical Mechanics: Theory and Experiment* **2016** 023202
- [14] Brandner K and Seifert U 2016 *Physical Review E* **93** 062134
- [15] Proesmans K and Fiore C E 2019 *Phys. Rev. E* **100**(2) 022141 URL <https://link.aps.org/doi/10.1103/PhysRevE.100.022141>
- [16] Martínez I A, Roldán É, Dinis L, Petrov D, Parrondo J M and Rica R A 2016 *Nature physics* **12** 67–70
- [17] Proesmans K, Dreher Y, Gavrilov M, Bechhoefer J and Van den Broeck C 2016 *Physical Review X* **6** 041010
- [18] Ciliberto S 2017 *Physical Review X* **7** 021051
- [19] Josefsson M, Svilans A, Burke A M, Hoffmann E A, Fahlvik S, Thelander C, Leijnse M and Linke H 2018 *Nature nanotechnology* **13** 920–924
- [20] Barato A C and Seifert U 2015 *The Journal of Physical Chemistry B* **119** 6555–6561
- [21] Pietzonka P, Barato A C and Seifert U 2016 *Physical Review E* **93** 052145
- [22] Gingrich T R, Horowitz J M, Perunov N and England J L 2016 *Physical review letters* **116** 120601
- [23] Seifert U 2018 *Physica A: Statistical Mechanics and its Applications* **504** 176–191
- [24] Proesmans K, Peliti L and Lacoste D 2018 A case study of thermodynamic bounds for chemical kinetics chemical kinetics beyond the textbook
- [25] Horowitz J M and Gingrich T R 2019 *Nature Physics* 1–6
- [26] Barato A C and Seifert U 2015 *Physical review letters* **114** 158101

- [27] Gingrich T R, Rotskoff G M and Horowitz J M 2017 *Journal of Physics A: Mathematical and Theoretical* **50** 184004
- [28] Li J, Horowitz J M, Gingrich T R and Fakhri N 2019 *Nature communications* **10** 1666
- [29] Manikandan S K, Gupta D and Krishnamurthy S 2019 *arXiv preprint arXiv:1910.00476*
- [30] Busiello D M and Pigolotti S 2019 *Physical Review E* **100** 060102
- [31] Pietzonka P and Seifert U 2018 *Physical Review Letters* **120** 190602
- [32] Hwang W and Hyeon C 2018 *The journal of physical chemistry letters* **9** 513–520
- [33] Pal S, Saryal S, Segal D, Mahesh T and Agarwalla B K 2019 *arXiv preprint arXiv:1912.08391*
- [34] Guioth J and Lacoste D 2016 *EPL (Europhysics Letters)* **115** 60007
- [35] Hasegawa Y and Van Vu T 2019 *Physical Review Letters* **123** 110602
- [36] Vroylandt H, Proesmans K and Gingrich T R 2019 *arXiv preprint arXiv:1910.01086*
- [37] Dechant A and Sasa S i 2018 *Journal of Statistical Mechanics: Theory and Experiment* **2018** 063209
- [38] Di Terlizzi I and Baiesi M 2018 *Journal of Physics A: Mathematical and Theoretical* **52** 02LT03
- [39] Barato A C and Seifert U 2016 *Physical Review X* **6** 041053
- [40] Ray S and Barato A C 2017 *Journal of Physics A: Mathematical and Theoretical* **50** 355001
- [41] Holubec V and Ryabov A 2018 *Physical review letters* **121** 120601
- [42] Proesmans K and Van den Broeck C 2017 *EPL (Europhysics Letters)* **119** 20001
- [43] Barato A C, Chetrite R, Faggionato A and Gabrielli D 2018 *New Journal of Physics* **20** 103023
- [44] Koyuk T, Seifert U and Pietzonka P 2018 *Journal of Physics A: Mathematical and Theoretical*
- [45] Proesmans K and Horowitz J M 2019 *Journal of Statistical Mechanics: Theory and Experiment* **2019** 054005
- [46] Barato A, Chetrite R, Faggionato A and Gabrielli D 2019 *Journal of Statistical Mechanics: Theory and Experiment* **2019** 084017
- [47] Koyuk T and Seifert U 2019 *Physical Review Letters* **122** 230601
- [48] Engel A 2009 *Physical Review E* **80** 021120
- [49] Nickelsen D and Engel A 2011 *The European Physical Journal B* **82** 207–218
- [50] Ryabov A, Dierl M, Chvosta P, Einax M and Maass P 2013 *Journal of Physics A: Mathematical and Theoretical* **46** 075002
- [51] Holubec V 2014 *Journal of Statistical Mechanics: Theory and Experiment* **2014** P05022
- [52] Rosas A, Van den Broeck C and Lindenberg K 2017 *Physical Review E* **96** 052135
- [53] Rosas A, Van den Broeck C and Lindenberg K 2018 *Physical Review E* **97** 062103
- [54] Šubr E and Chvosta P 2007 *Journal of Statistical Mechanics: Theory and Experiment* **2007** P09019
- [55] Chvosta P, Holubec V, Ryabov A, Einax M and Maass P 2010 *Physica E: Low-dimensional Systems and Nanostructures* **42** 472–476
- [56] Verley G, Van den Broeck C and Esposito M 2013 *Physical Review E* **88** 032137
- [57] Herrmann S and Landon D 2015 *Stochastics and Dynamics* **15** 1550022
- [58] Van den Broeck C and Toral R 2015 *Physical Review E* **92** 012127
- [59] Schnakenberg J 1976 *Reviews of Modern physics* **48** 571
- [60] Callen H B 1998 *Thermodynamics and an introduction to thermostatistics*
- [61] De Groot S R and Mazur P 2013 *Non-equilibrium thermodynamics* (Courier Corporation)
- [62] Touchette H 2009 *Physics Reports* **478** 1–69
- [63] Koyuk T and Seifert U 2020 *arXiv preprint arXiv:2005.02312*
- [64] Potts P P and Samuelsson P 2019 *Physical Review E* **100** 052137